Journal of Magnetism and Magnetic Materials 320 (2008) 2714–2720

Contents lists available at ScienceDirect

Journal of Magnetism and Magnetic Materials

journal homepage: www.elsevier.com/locate/jmmm

Magneto-dielectric properties of polymer–Fe_3O_4 nanocomposites

Ta-I Yang [a], Rene N.C. Brown [a], Leo C. Kempel [b], Peter Kofinas [c,*]

[a] Department of Chemical and Biomolecular Engineering, University of Maryland, College Park, MD 20742, USA
[b] Department of Electrical and Computer Engineering, Michigan State University, East Lansing, MI 48824, USA
[c] Fischell Department of Bioengineering, University of Maryland, 1120 Jeong H. Kim Building, College Park, MD 20742, USA

ARTICLE INFO

Article history:
Received 18 December 2007
Received in revised form
4 March 2008
Available online 12 June 2008

Keywords:
Iron oxide
Composite
Magneto-dielectric

ABSTRACT

The aim of this research is to elucidate the size effect of magnetic nanoparticles on the resultant magneto-dielectric properties of polymer nanocomposites at radio frequencies. The block copolymer of [styrene-b-ethylene/butylene-b-styrene] (SEBS) was utilized as a matrix for the templating of magnetic nanoparticles. Surfactant-modified iron oxide (Fe_3O_4) nanoparticles of various sizes were successfully synthesized by a seed-mediated growth method. The surfactant prevented Fe_3O_4 aggregation and provided compatibility with the polymer matrix. The nucleation and growth of Fe_3O_4 nanoparticles was controlled by changing the concentration ratio of surfactant to iron-precursor. The free iron ions present during synthesis are the major factor contributing to the growth of larger particles. The Fe_3O_4 nanoparticle critical size for superparamagnetic to ferrimagnetic transition was determined to be near 30 nm at room temperature. The dielectric permittivity (ε_r) of the polymer composite increased with increasing amount of Fe_3O_4 doping, and was not influenced by nanoparticle size. However, the magnetic permeability (μ_r) of the composites was significantly influenced by the size of Fe_3O_4 nanoparticles templated within the block copolymer matrix due to thermal energy fluctuations from the nanoparticle surroundings.

1. Introduction

Materials having a wide range of magneto-dielectric properties are promising for advanced applications in microwave communication devices and their miniaturization [1–3]. Such magneto-dielectric materials must exhibit not only a high relative dielectric permittivity (ε_r) which allows the size of a microwave device to be scaled by $\varepsilon_r^{-1/2}$ [1], but also the appropriate ratio of relative permittivity (ε_r) to relative magnetic permeability (μ_r) [2–5]. For example, the bandwidth for antenna applications could be improved by a factor of 13, when the μ_r/ε_r ratio is equal to 3, while keeping the product $\mu_r \cdot \varepsilon_r = 25$ [3]. In addition, the weight, shape-flexibility, and ease of processing of the material are also key factors for their application. That is the main reason why many research efforts have focused on polymer composites. Most studies to date have employed the conventional approach of blending magnetic particles into polymers [6–8]. Such methods lack control on particle size and distribution within the polymer matrix due to the intrinsic incompatibility between inorganic particles and organic matrices. However, it has been shown in literature that the characteristic length (surface-to-volume ratio) of nanoparticles, and their distribution and effective volume fraction in the polymer composites will significantly influence their dielectric [9–12] and magnetic properties [13–15]. Specifically for magnetic nanoparticles, their magnetization significantly depends on particle characteristic length [16]. As the size of the magnetic particles is reduced from the bulk, only single magnetic domains without any domain walls exist in particles below a certain critical size (D_{SD}). Furthermore, the particles become superparamagnetic when the anisotropy energy cannot sustain the magnetization of the particles due to thermal energy effects. Superparamagnetism can be overcome by reducing the system's temperature, increasing particle size, or increasing the shapeanisotropy (e.g., irregular particle shape results in larger shape anisotropy) [17].

In order to elucidate the effect of characteristic length and volume fraction of particles on the resultant magneto-dielectric properties of the polymer nanocomposites, surface-modified magnetic nanoparticles have been considered. The size and shape of the surface-modified nanoparticles are controllable by introducing amphiphilic surfactants or ionic polymers during synthesis [18], which possess hydrophilic and hydrophobic components. The polar groups in the hydrophilic component can associate with the nanoparticle surface and passivate the high energy surface of the nanoparticle. The bulky hydrophobic component provides steric isolation needed to prevent van der Waals and magnetic attractions among magnetic particles, which is the cause of

* Corresponding author. Tel.: +1 301 405 7335; fax: +1 301 314 6868.
E-mail address: kofinas@umd.edu (P. Kofinas).
URL: http://www.glue.umd.edu/~kofinas (P. Kofinas).

0304-8853/$ - see front matter © 2008 Elsevier B.V. All rights reserved.
doi:10.1016/j.jmmm.2008.06.008

nanoparticle agglomeration. Moreover, surface-modified nanoparticles can dissolve in polar solvents [19] or non-polar solvents [20–22], depending on the chemical affinity of the bulky component of the surfactant to these solvents. Many studies have shown that Fe [21], $CoFe_2O_4$ [23], Fe_3O_4 [22,23], and γ-Fe_2O_3 [24] magnetic nanoparticles with narrow size distribution and no agglomeration can be synthesized with modifying surfactants. However, such nanoparticles are superparamagnetic, which means that the particles are easily demagnetized by thermal fluctuations from the environment they are in.

In this study we investigated the particle size effect on magneto-dielectric properties of Fe_3O_4/polymer composites at radio frequencies (1 M to 1 GHz). Surface-modified iron oxide (Fe_3O_4) nanoparticles were synthesized using a sodium oleate surfactant to improve compatibility with the polymer matrix. The size of the nanoparticles was tailored by a seed-mediated method, which utilizes smaller nanoparticles as growth sites to synthesize larger particles. A possible mechanism for the nucleation and growth of Fe_3O_4 particles will be discussed. The dielectric (ε_r) and magnetic (μ_r) properties of the resulting nanocomposites consisting of various particles dispersed in polymer matrices were measured using impedance analysis.

2. Experimental section

Materials: Sodium oleate (97%) was purchased from TCI America. Iron(III) chloride (97%), oleic acid (90%), and 1-octadecene (90%) were purchased from Aldrich. The block copolymer of [styrene-b-ethylene/butylene-b-styrene] (SEBS) was supplied by Kraton Polymers. All chemicals were used as received.

Synthesis of 11 *nm*Fe_3O_4 *nanoparticle seeds*: The procedure for synthesizing the surfactant-modified iron oxide nanoparticles is similar to what has been reported in literature [22]. $FeCl_3$ (10.8 g) and sodium oleate (36.5 g) were reacted in a mixed solvent (80 ml ethanol, 60 ml distilled water, and 140 ml hexane) at 70 °C for 4 h. The upper organic layer containing the iron–oleate complex (Fe-precursor) was washed three times with 30 ml distilled water and then dried. The resulting iron–oleate complex was added to 200 ml of 1-octadecene mixed with oleic acid (5.7 g). The mixture was heated to 320 °C in an argon atmosphere. After 30 min at 320 °C, the solution turned black and was then cooled down to room temperature. Ethanol was added to precipitate the surfactant-coated iron oxide particles. The precipitated particles were centrifuged to remove any residual solvents.

Synthesis of Fe_3O_4 *nanoparticles via* 11 *nm* (Fe_3O_4) *seeds*: The 11 nm Fe_3O_4 nanoparticles were used as growth seeds to obtain larger particles. The amounts of iron–oleate complex (Fe-precursor), oleic acid, and seeds were systematically varied and their effect on resulting nanoparticle size was studied. All components were added into a solvent (1-octadecene) and heated to 320 °C for 3 h. After cooling to room temperature and adding excess ethanol, surfactant-coated iron oxide particles were recovered from the solvent.

Preparation of Fe_3O_4 *nanocomposites*: Fe_3O_4/polymer nanocomposites were prepared using a solution-casting method, since both surfactant-modified Fe_3O_4 and polymer dissolve in a common solvent, tetrahydrofuran (THF). The modified Fe_3O_4 particles and polymer (SEBS) were dissolved in THF and mixed for 1 h, then a film was statically cast over a period of one day.

Characterization: Transmission electron microscopy (TEM, HITACHI H-600 or JEOL 200CX) was used to observe the morphology of the nanoparticles. Samples for TEM were prepared by evaporating a dilute Fe_3O_4 THF solution on a carbon-coated grid. The particle size is reported as the average size (D_{avg}), which is the average particle size of approximately 1000 individual particles from TEM images. Magnetic properties were investigated using superconducting quantum interference device (SQUID) magnetometry. Samples for SQUID measurements consisted of approximately 10 wt% of iron oxide particles and their weight were in the 15 mg range. The form of the samples was cubic geometry (2 mm × 2mm × 2 mm). The amount of iron oxide inside the polymer matrix was determined using thermogravimetric analysis (TGA-50, SHIMADZU) in nitrogen atmosphere. The polymer and surfactant were burnt out and only iron oxide particles remained without change in the crystalline structure. The magneto-dielectric properties (relative dielectric permittivity, ε_r, and relative magnetic permeability, μ_r) in the 1 MHz to 1 GHz range were measured using an Agilent RF impedance/material analyzer (E4991A). Samples for ε_r measurement were prepared in the shape of a solid disc with a diameter of 0.75″ and a thickness of 0.1″. Samples for μ_r measurement were in the geometry of a washer with an outer diameter of 0.75″, an empty inner diameter of 0.25″, and a thickness of 0.1″.

3. Results and discussion

3.1. Structural characterization of 11 nm Fe_3O_4 seeds

The nanoparticle seeds used in the seed-mediated growth studies were spherical with narrow size distribution, as shown in Fig. 1. The average size (D_{avg}) measured from TEM was 11.3 ± 0.3 nm. Fig. 2 depicts a selected area electron diffraction pattern from the synthesized nanoparticles in Fig. 1a and shows

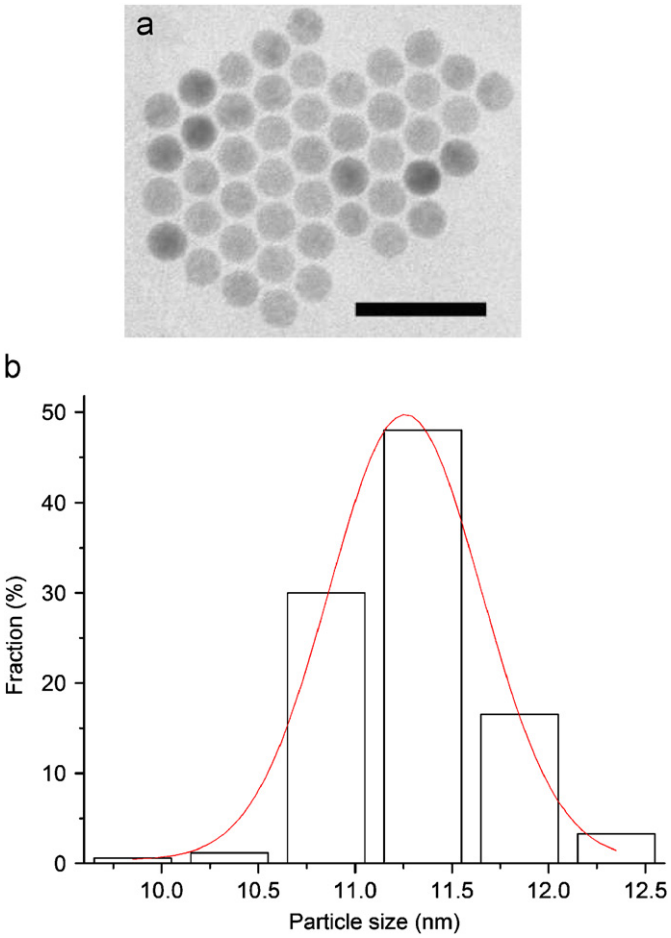

Fig. 1. (a) TEM image of surfactant-modified Fe_3O_4 nanoparticles (scale bar = 50 nm); (b) particle size distribution.

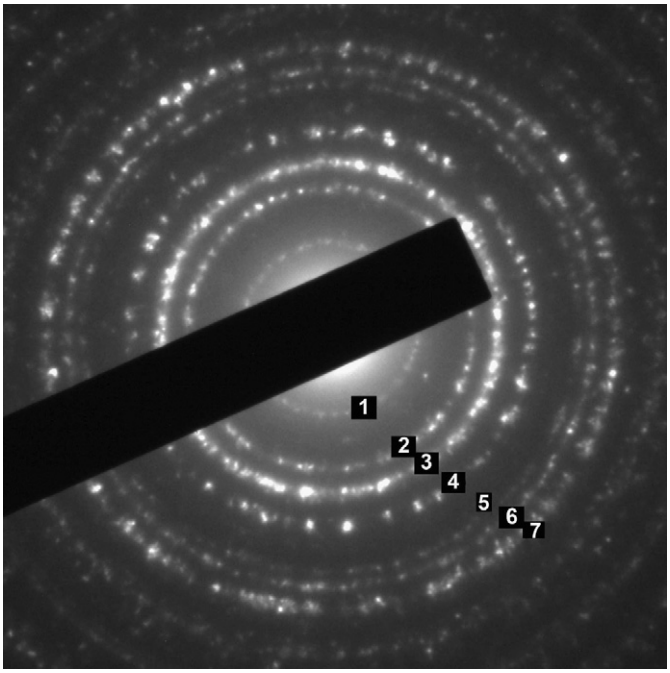

Fig. 2. Selected area electron diffraction pattern of Fe_3O_4 nanoparticles.

Table 1
Lattice spacing of Fe_3O_4, d (Å), derived from the diffraction pattern shown in Fig. 2

Ring	1	2	3	4	5	6	7
d	4.85	2.98	2.53	2.10	1.72	1.62	1.50
hkl	111	220	311	400	422	511	440

multiple diffraction rings. The calculated lattice d-spacings derived from the diffraction rings is consistent with bulk or nano-size magnetite (Fe_3O_4) reported in literature [23,25], as given in Table 1. The chemical composition of Fe_3O_4 was also confirmed by comparing the properties of as-synthesized particles and their heat-transformed form, γ-Fe_2O_3. However, the majority of the synthesized nanoparticle composition should be Fe_3O_4 with a small percentage of γ-Fe_2O_3, as reported in literature [22].

3.2. *Mechanism of* Fe_3O_4 *formation by seed-mediated growth*

In the classic LaMer mechanism [26], the formation of colloids from homogenous solution occurs when the precursor concentration is above the supersaturated limit. Further growth of the nuclei is spontaneous but limited by diffusion of the precursor to the nucleus surface. In our nanoparticle synthesis system, iron ions were released by dissociation from the iron–oleate complex at 320 °C [22]. When the Fe^{3+} ion concentration in solution overcame the supersaturation limit, Fe_3O_4 particle nucleation took place and subsequently the nuclei grew and stabilized at an approximate size of 11 nm within 30 min at 320 °C [22]. Even though the reaction was continued for 10 h, no particle growth was observed by Ostwald ripening [24]. Therefore, the seed-mediate d method was utilized in order to obtain larger particles [23,27]. The original synthesized Fe_3O_4 nanoparticle seeds were used as nuclei to grow larger Fe_3O_4 particles and the influence of surfactant/precursor and seed size on magneto-dielectric properties was investigated [24,28,29].

Surfactant and Fe-*precursor*: sample 1 indicated that Fe_3O_4 nanoparticles did not grow to a larger size as expected by the amount of seeds added, when the concentration ratio of oleic acid

Table 2
Effect of surfactant concentration on average particle size (D_{avg})

Sample	S/Fe	[seed] (g/L)	D_{avg} (nm)
Seed	0.5	0	11.3 ± 0.3
1	2	3.2	10.1 ± 0.6
2	2	7.9	9.8 ± 0.8
3	4	3.2	0

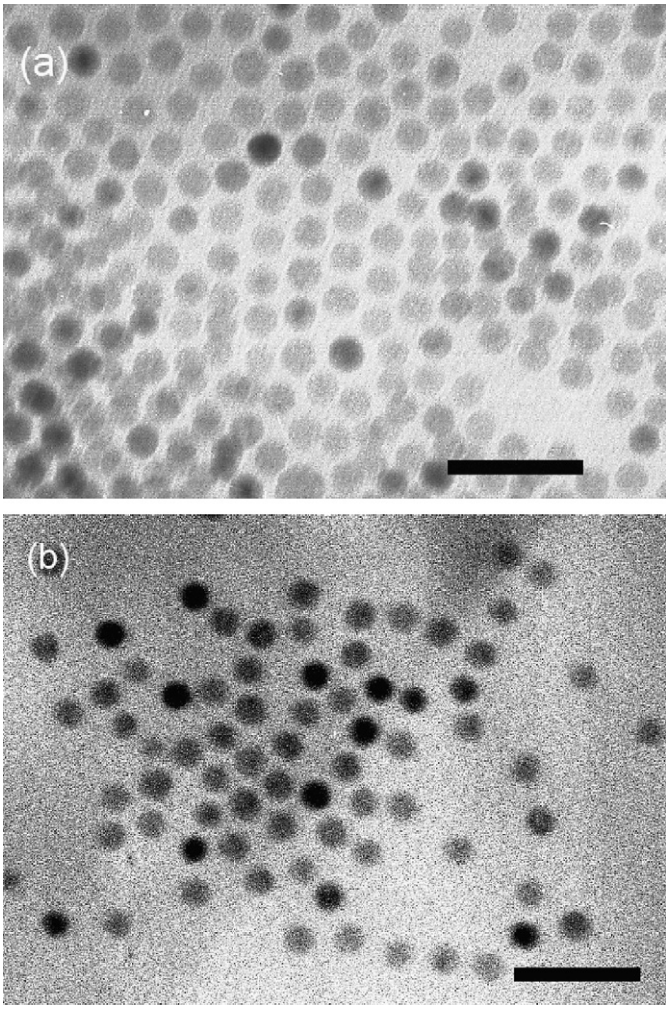

Fig. 3. TEM images of high S/Fe nanoparticles: (a) sample 1 and (b) sample 2 (scale bar = 50 nm).

surfactant to Fe-precursor (S/Fe) was 2 and 3.2 g/L of seeds was used (see Table 2 and Fig. 3). The same particle distribution between samples 1 and 2 also indicates that the Fe_3O_4 nucleation rate from solution was faster than the nuclei growth rate although the seed concentration was doubled when the S/Fe ratio was kept at 2. At higher surfactant concentration (S/Fe = 4), no Fe_3O_4 particles were formed, which is consistent with literature reports that excess surfactant impedes the formation of Fe_3O_4 particles [24,29]. Asthe ratio S/Fe decreased from 2 to 0.5, the average particle size (D_{avg}) increased as shown in Fig. 4 and Table 3. However, D_{avg} decreased again at a ratio S/Fe of 0.25 (sample 6 in Table 3). These results suggest that extremely low surfactant concentrations have an adverse effect on particle growth from nuclei although modest surfactant present in solution promotes Fe_3O_4 formation in favor of particle growth. To further investigate the effect of less surfactant on nanoparticle growth, the particle synthesis was conducted without adding surfactant (sample 7 in

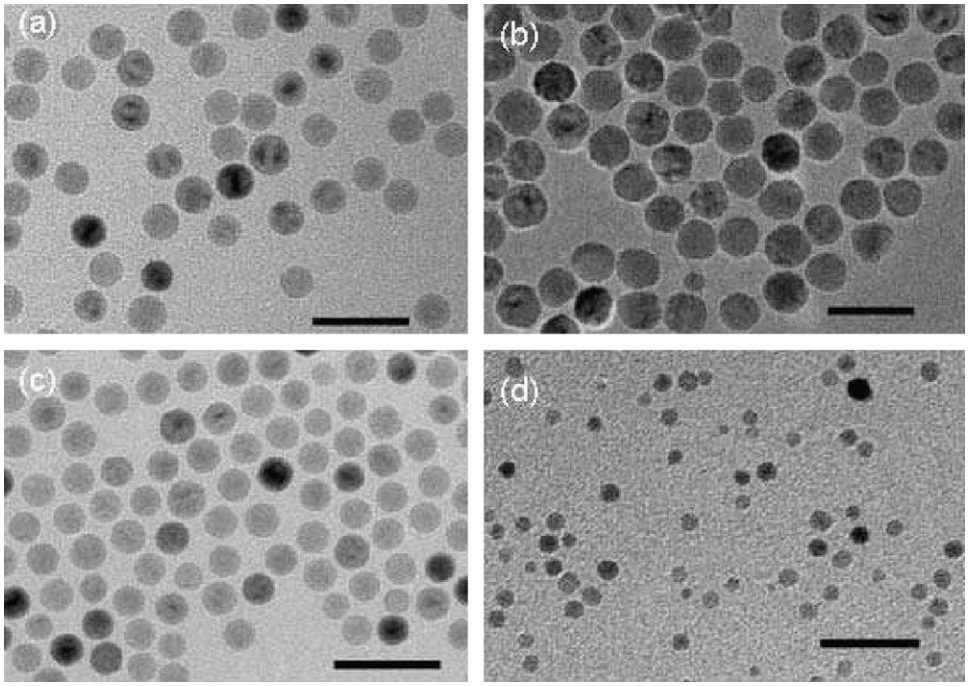

Fig. 4. TEM images of low S/Fe nanoparticles: (a) sample 4; (b) sample 5; (c) sample 6; (d) sample 7 (scale bar = 50 nm).

Table 3
Effect of surfactant concentration on average particle size (D_{avg})

Sample	S/Fe	[seed] (g/L)	D_{avg} (nm)
4	1	7.9	18.4 ± 2.1
5	0.5	7.9	22.2 ± 4.5
6	0.25	7.9	13.9 ± 1.7
7	0	7.9	10.1 ± 2.1

Table 3). In addition, an excess of oleylamine was added into the solution in order to reduce the reactivity of oleate surfactant present in the Fe-precursor and seeds. It is well known that carboxylic acid (–COOH) groups of oleate surfactants tend to associate with amine groups ($-NH_2$) of oleylamine instead of associating with the Fe^{3+} ions or the Fe_3O_4 nanoparticle surface [20,30]. The observed D_{avg} of 10.1 nm with high standard deviation (±2.1 nm) confirms that less surfactant leads to formation of smaller particles (Fig. 4d). Overall, the effect of the ratio S/Fe on particle size distribution can be summarized in Fig. 5. The optimal ratio (S/Fe) is 0.5 for growing larger particles. Two distinct regions can be found in which the particle size decreases with decreasing (Region I) or increasing S/Fe (Region II), respectively. These results can be explained by the free Fe^{3+} ions present in the solution (Fe_{free}). Fe_{free} is the amount of Fe^{3+} ions not associated (trapped) by surfactants, which freely participates in Fe_3O_4 formation. In Region I, less surfactant or more iron-precursor (lower S/Fe) results in higher Fe_{free} to overcome the supersaturation limit for nucleating Fe_3O_4 nanoparticles fromhomogeneous solution. Fe_{free} ions were consumed for nucleating small particles (nucleation domination) instead of diffusing to nuclei for nanoparticle growth as shown in Fig. 6. In Region II, Fe_3O_4 nucleation dominated with increased $R_{S/Fe}$. As shown in Fig. 7, once Fe_{free} ions were released from the iron–oleate complex, they re-associated with surfactants already present in the solution. Therefore, higher surfactant concentrations promoted Fe_{free} ion localization and hindered their diffusion into stable nuclei for particle growth. Consequently, Fe_3O_4 nucleated to smaller nuclei instead of growing to larger

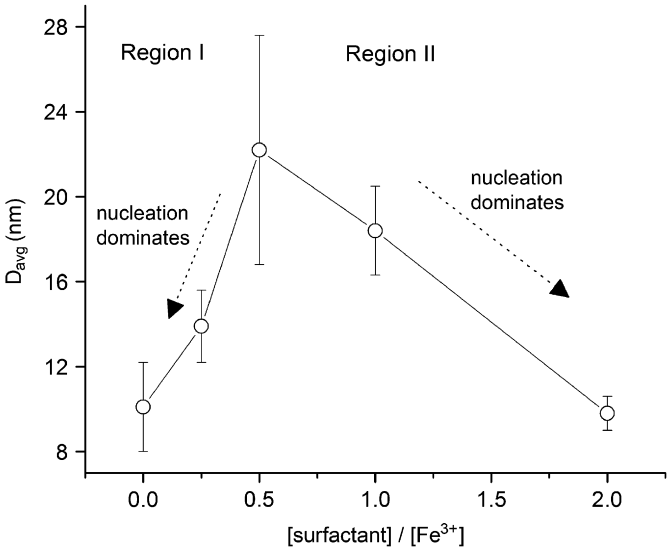

Fig. 5. Effect of S/Fe on Fe_3O_4 particle size distribution.

particle sizes. No Fe_3O_4 nanoparticles formed, because most Fe_{free} ions were captured at extremely high surfactant concentration (sample 3 in Table 2).

Seed size: The seed size effect on Fe_3O_4 nanoparticle formation was studied by utilizing sample 5 as the seed. The resulting Fe_3O_4 nanoparticles (sample 8) grew to a larger size (26.2 ± 7.6 nm) from the original 22.2 ± 4.5 nm, as shown in Fig. 8. The smaller growth extent from 22.2 to 26.2 nm indicates that larger particles have a slower growth rate compared to smaller particles (compared to sample 5 which was seeded by 11 nm seeds) [28]. The particle size distribution of sample 5 (Fig. 9) was polydisperse because neither the nucleation nor the growth step was suppressed during Fe_3O_4 formation although seeds were monodisperse (Fig. 1b). Sample 8 exhibited a similar behavior, i.e. the particle growth step did not dominate, leading to a bimodal particle distribution as shown in Fig. 9b.

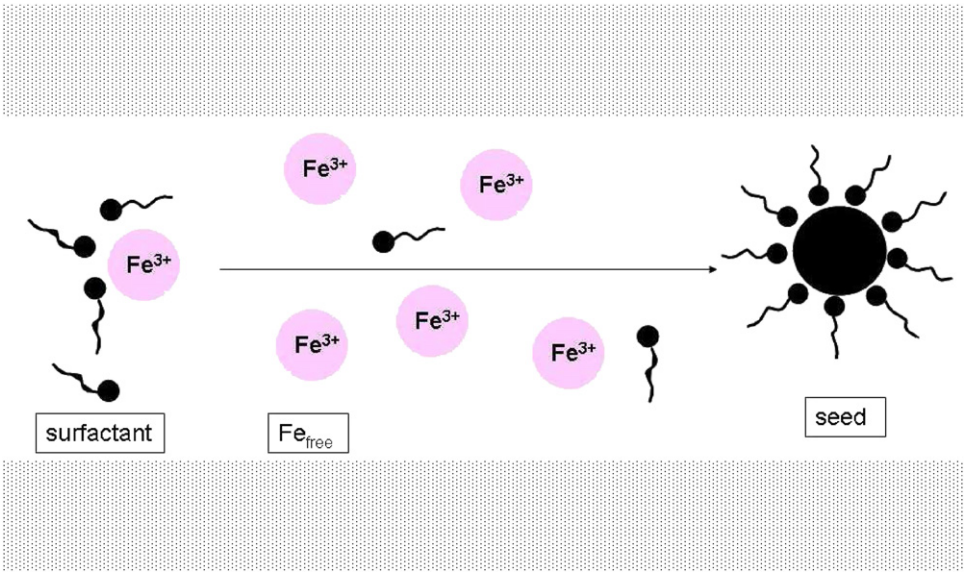

Fig. 6. Effect of low S/Fe on Fe_3O_4 nanoparticle formation.

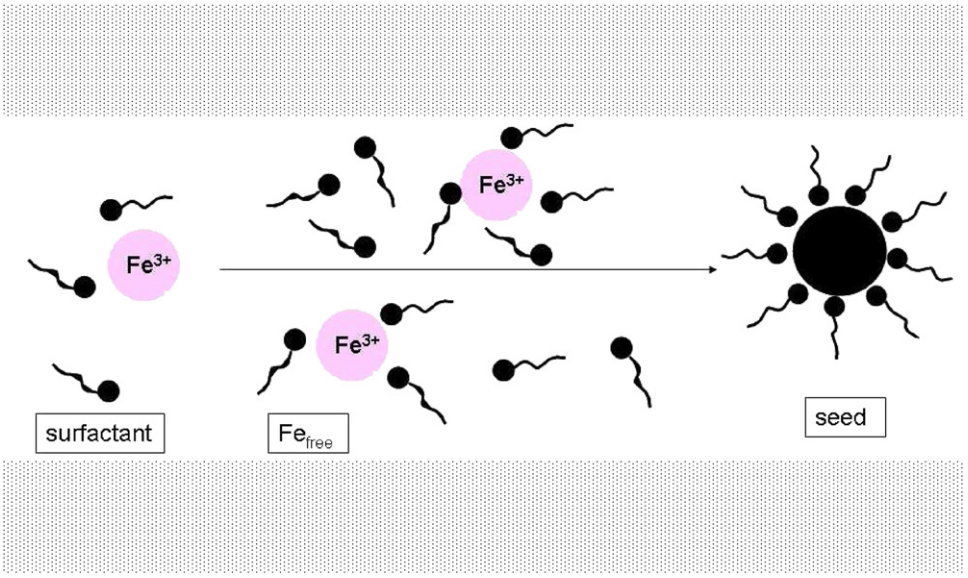

Fig. 7. Effect of high S/Fe on Fe_3O_4 nanoparticle formation.

3.3. *Magnetic properties of* Fe_3O_4 *nanoparticles*

Fig. 10 shows the room temperature magnetization as a function of applied magnetic field for samples 5 and 8. There is hysteresis present for sample 8 with a coercivity (H_c) of 50 Oe, which is consistent with ferrimagnetic behavior. The D_{avg} of 26.2 ± 7.6 below the 50–60 nm critical limit (D_{SD}) for Fe_3O_4 single magnetic domains suggests that sample 8 did not consist of magnetic multi-domains [31]. The weaker H_c (50 Oe) compared to 200 Oe obtained from the 70 nm Fe_3O_4 nanoparticles contributes to thermal effects in the single-domain region [32]. This means that the thermal energy provided from the nanoparticle surroundings significantly reduced the particle magnetization sustained by the anisotropy energy (KV), which is weaker for smaller particle sizes [17]. There is a small hysteresis ($H_c = 5$ Oe) observed for sample 5 as shown in the insert of Fig. 10. It has been reported in the literature that the Fe_3O_4 critical size (D_{SP}) for superparamagnetic to ferrimagnetic transition lies between 25 and 30 nm [31]. As shown in Fig. 9a, 40% and 10% of the number of nanoparticles in sample 5 are larger than 25 and 30 nm, respectively. Therefore, it could be concluded that the D_{SP} is near 30 nm, since the small observed coercivity (5 Oe) should arise from the lower amount of nanoparticles present. The D_{SP} of 30 nm is not generally accurate for pure Fe_3O_4 since the synthesized nanoparticles were non-stoichiometric Fe_3O_4. However, it provides valuable evidence for confirming the accurate D_{SP} of Fe_3O_4 which lies near 30 nm. It was also observed that the saturation magnetization (M_s) of samples 5 and 8 is lower than the bulk value of Fe_3O_4 (90 emu/g) due to spin disorder arising from the larger particle surface area (smaller particle) as suggested in literature [33].

3.4. *Magneto-dielectric properties of the* Fe_3O_4*–polymer composites*

The measured relative dielectric permittivity (ε_r) and magnetic permeability (μ_r) values of the polymer composites with

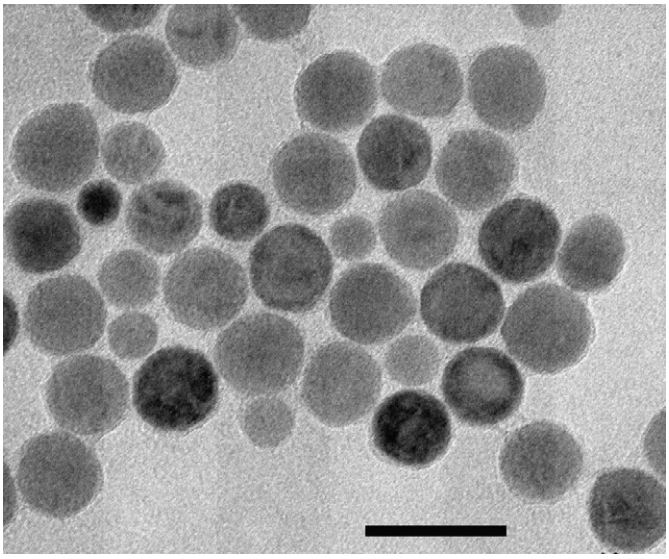

Fig. 8. TEM image of Fe_3O_4 nanoparticles (sample 8) synthesized with the same conditions as sample 5, except using sample 5 as seeds (scale bar = 50 nm).

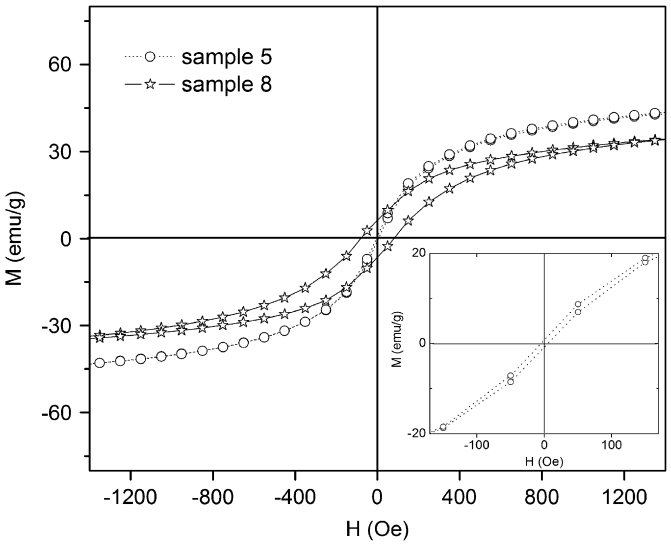

Fig. 10. Magnetization (M) vs applied magnetic field (H) for samples 5 and 8 at 300 K.

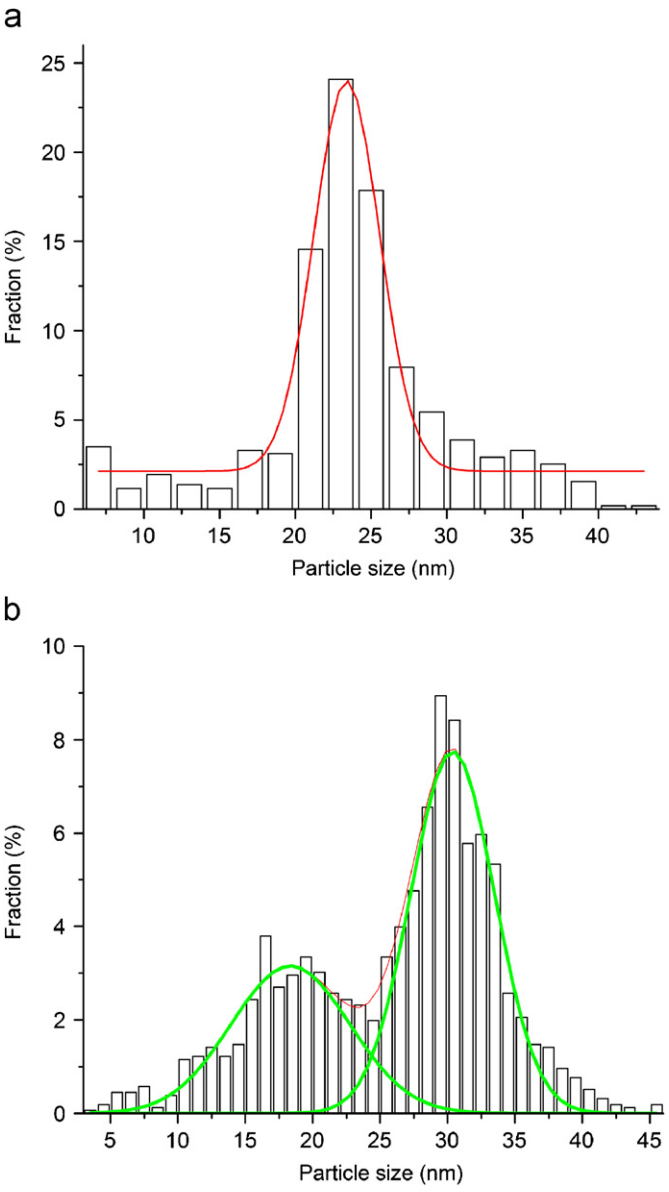

Fig. 9. Particle distribution of: (a) sample 5 (seeds for sample 8); (b) sample 8.

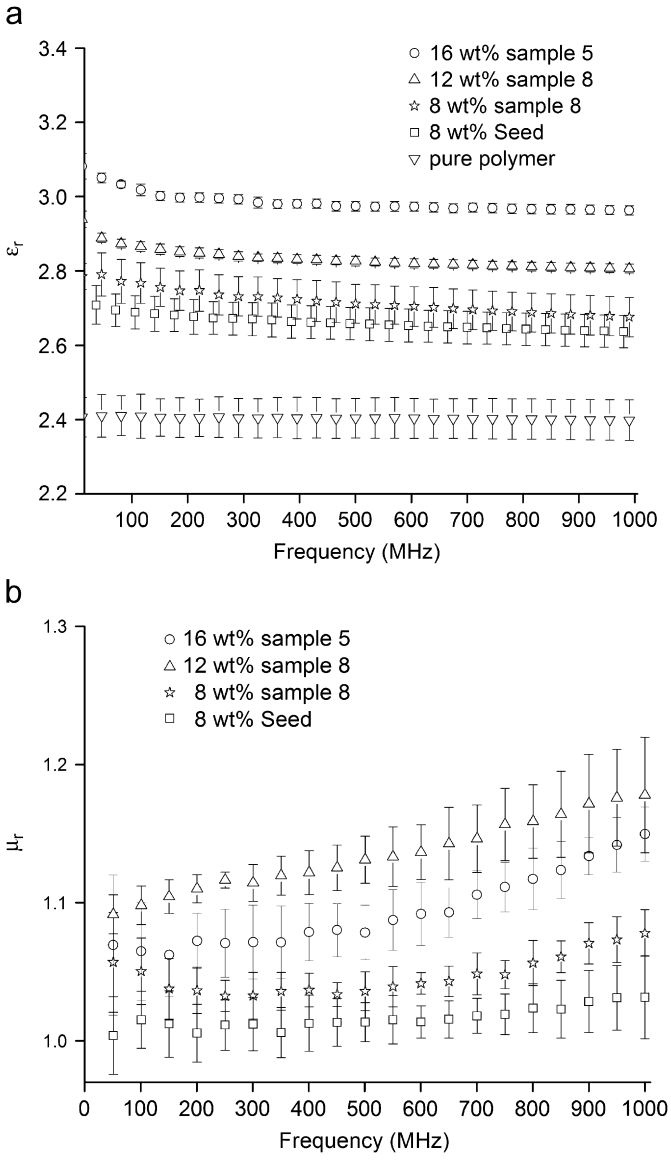

Fig. 11. High frequency relative permittivity (ε_r) and magnetic permeability (μ_r) of surfactant-modified Fe_3O_4 nanocomposites at room temperature.

surfactant-modified Fe_3O_4 nanoparticles are shown in Fig. 11. The ε_r of the polymer composite (SEBS) ($\varepsilon_r = 2.4$) improved from 2.4 to 3.0 with increasing amount of Fe_3O_4 nanoparticle doping. Sample 8 and the nanoparticle sample used to seed the growth of larger particle sizes, which have the highest size difference (from 11.1 to 26.2 nm), show the same value of ε_r. This indicates that particle size does not affect the dielectric permittivity (ε_r) of the polymer composites. However, the μ_r of the SEBS polymer composite ($\mu_r = 1$) did not always increase with addition of Fe_3O_4 nanoparticles. The composite with 8 wt% of 11 nm Fe_3O_4 (seed) showed the same μ_r of 1 as the pure SEBS polymer. This suggests that the thermal energy provided by the particle surroundings significantly lowers the magnetization of the polymer composite since the 11 nm Fe_3O_4 nanoparticles are superparamagnetic. For composites with single-domain Fe_3O_4 nanoparticles (samples 5 and 8), higher μ_r values were obtained with smaller amounts of larger size particles (sample 8). This is because larger particles result in higher anisotropy energies (*KV*), which is needed to overcome the demagnetization arising from thermal energy effects. Therefore, a larger particle size is one of the major contributing factors required to maintain the particle's magnetization and to obtain higher values of μ_r when the particle size is within the magnetic single-domain region.

4. Conclusions

We have demonstrated the feasibility of a seed-mediated method to synthesize surfactant-modified Fe_3O_4 nanoparticles with various particle distributions. The surfactant and Fe-precursor play a crucial role in determining the particle nucleation and growth rate and lead to different nanoparticle sizes. In addition, the size of the seeds also led to different Fe_3O_4 growth extent and particle distributions because both nucleation and growth steps occurred during synthesis. The dielectric permittivity (ε_r) of the polymer nanoparticle composite increased by adding surfactant-modified Fe_3O_4 nanoparticles, and particle size did not significantly influence ε_r. However, higher magnetic permeabilities (μ_r) were obtained using larger Fe_3O_4 nanoparticles. This is because a higher anisotropy energy (*KV*) can overcome thermal effects from the particle surroundings and sustain a high magnetization.

Acknowledgments

This material is based upon work supported by the Air Force Office of Scientific Research, Grant # FA95500610097.

References

[1] T. Siegrist, T.A. Vanderah, Eur. J. Inorg. Chem. 2003 (2003) 1483.
[2] N.E. Kazantseva, N.G. Ryvkina, I.A. Chmutin, J. Commun. Technol. Electron. 48 (2003) 173.
[3] A. Buerkle, K. Sarabandi, IEEE Trans. Antennas Propag. 53 (2005) 3436.
[4] H. Mosallaei, K. Sarabandi, IEEE Trans. Antennas Propag. 52 (2004) 1558.
[5] S.S. Kim, S.B. Jo, K.I. Gueon, K.K. Choi, J.M. Kim, K.S. Chum, IEEE Trans. Magn. 27 (1991) 5462.
[6] P. Singh, V.K. Babbar, A. Razdan, R.K. Puri, T.C. Goel, J. Appl. Phys. 87 (2000) 4362.
[7] Y.J. Chen, M.S. Cao, T.H. Wang, Q. Wan, Appl. Phys. Lett. 84 (2004) 3367.
[8] K.M. Lim, K.A. Lee, M.C. Kim, C.G. Park, J. Non-Cryst. Solids 351 (2005) 75.
[9] J.W. Wang, Q.D. Shen, C.Z. Yang, Q.M. Zhang, Macromolecules 37 (2004) 2294.
[10] C.W. Nan, Prog. Mater. Sci. 37 (1993) 1.
[11] P.S. Neelakanta, Handbook of Electromagnetic Materials: Monolithic and Composite Versions and Their Applications, CRC Press, Boca Raton, FL, 1995, p. 133.
[12] E. Tuncer, Y.V. Serdyuk, S.M. Gubanski, IEEE Trans. Dielectr. Electr. Insul. 9 (2002) 809.
[13] C. Kittel, Phys. Rev. 70 (1946) 965.
[14] R.H. Kodama, J. Magn. Magn. Mater. 200 (1999) 359.
[15] B.W. Li, Y. Shen, Z.X. Yue, C.W. Nan, J. Magn. Magn. Mater. 313 (2007) 322.
[16] M.A. Willard, L.K. Kurihara, E.E. Carpenter, S. Calvin, V.G. Harris, Int. Mater. Rev. 49 (2004) 125.
[17] N.A. Spaldin, Magnetic Materials: Fundamentals and Device Applications, Cambridge University Press, New York, 2003 (Chapters 10–11).
[18] B.L. Cushing, V.L. Kolesnichenko, C.J. O'Connor, Chem. Rev. 104 (2004) 3893.
[19] K.C. Huang, S.H. Ehrman, Langmuir 23 (2007) 1419.
[20] D. Farrell, S.A. Majetich, J.P. Wilcoxon, J. Phys. Chem. B 107 (2003) 11022.
[21] D. Farrell, Y. Cheng, R.W. McCallum, M. Sachan, S.A. Majetich, J. Phys. Chem. B 109 (2005) 13409.
[22] J. Park, K.J. An, Y.S. Hwang, J.G. Park, H.J. Noh, J.Y. Kim, J.H. Park, N.M. Hwanga, T. Hyeon, Nat. Mater. 3 (2004) 891.
[23] S. Sun, H. Zeng, D.B. Robinson, S. Raoux, P.M. Rice, S.X. Wang, G. Li, J. Am. Chem. Soc. 126 (2004) 273.
[24] M. Yin, A. Willis, F. Redl, N.J. Turro, S.P. O'Brien, J. Mater. Res. 19 (2004) 1208.
[25] R.M. Cornell, U. Schwertmann, The Iron Oxides: Structure, Properties, Reactions, Occurrence and Uses, Wiley-VCH, Weinheim, 2003, p. 175.
[26] M.A. Watzky, R.G. Finke, J. Am. Chem. Soc. 119 (1997) 10382.
[27] M.A. Watzky, R.G. Finke, Chem. Mater. 9 (1997) 3083.
[28] J.T.G. Overbeek, Adv. Colloid Interface. 15 (1982) 251.
[29] W.W. Yu, J.C. Falkner, C.T. Yavuz, V.L. Colvin, Chem. Commun. 20 (2004) 2306.
[30] A.G. Roca, M.P. Morales, C.J. Serna, IEEE Trans. Magn. 42 (2006) 3025.
[31] D.J. Dunlop, Phys. Earth Planet. Inter. 26 (1981) 1.
[32] S. Arajs, N. Amin, E.E. Anderson, J. Appl. Phys. 69 (1991) 5122.
[33] G.F. Goya, T.S. Berquo, F.C. Fonseca, M.P. Morales, J. Appl. Phys. 94 (2003) 3520.